

TUNING THE MATSUDA VOLTAGE OF THE TRIFT SPECTROMETER

to Optimize the Mass Accuracy for Peak Identification

OVERVIEW

A vital characteristic of time-of-flight secondary ion mass spectrometry (TOF-SIMS) is the capability to visualize chemical information in a spatially resolved manner. The ability to uniquely identify a peak in the mass spectrum and to elucidate its composition is an equally essential function of TOF-SIMS. Peak identification is strongly dependent on the mass resolving power and mass accuracy of the spectrometer. Of similar importance is the linearity of the mass scale over a large mass range for a given calibration.

In this Bulletin, we demonstrate both the importance of and the method for tuning the Matsuda voltage of the TRIFT mass spectrometer in order to optimize the mass accuracy for a common mass spectral calibration. The Matsuda is comprised of plates above and below the second ESA of the TRIFT analyzer for fine field

shaping to achieve superior compensation of the initial secondary ion kinetic energy dispersion [1]. The mass accuracy of the TRIFT is specified as less than 2 mamu for the mass range below 100 m/z and less than 10 ppm for the mass range above 100 m/z , and this level of performance is easily achieved with proper tuning of the Matsuda voltage.

A difficulty is often encountered in mass spectrometry because atomic and elemental species have a broader kinetic energy distribution than do polyatomic and molecular species [2,3]. These differences in kinetic energy distribution are illustrated in Figure 1. The TRIFT analyzer is designed with specific advantages for kinetic energy focusing, and differences in the kinetic energy distribution between atomic and molecular species are compensated such that nearly equivalent mass accuracy may be achieved. It is also demonstrated that mass

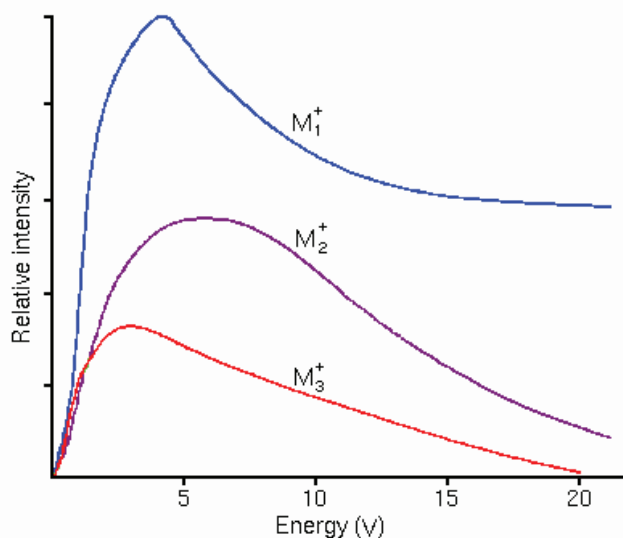


Figure 1: Illustration of the differences in kinetic energy distribution arising from different secondary ion (SI) species. The blue curve represents the distribution of an atomic SI species, M_1^+ ; the purple curve represents the distribution of a dimer SI species, M_2^+ ; the red curve represents the distribution of a trimer SI species, M_3^+ . Note that saturated organic SI species, i.e. those containing multiple H atoms, usually have a kinetic energy distribution of less than 5 eV.

resolution is affected only slightly by changes in the Matsuda voltage. Thus, high mass accuracy and mass resolution may be achieved simultaneously for both atomic and molecular secondary ions.

EXPERIMENTAL

The sample used for this test procedure should be a nominally flat piece of steel. Alternative samples may be used, but the specific secondary ions that are monitored for mass accuracy will necessarily be different. Most samples, independent of composition, will have some amount of adventitious hydrocarbon contamination which may be used for mass spectral calibration. The liquid metal ion gun (LMIG) should be used with the 200 μm aperture (1.5 nA DC current) setting and with a 100 – 200 μm field-of-view (FOV). Mass spectra should be acquired using the 240 eV (open) energy slit setting, and with the Contrast Diaphragm in the Out position (i.e. CD-Out). Ensure that both the sample Z-height and the sample bias are correct. The mass spectra should be calibrated using the fully saturated, low mass hydrocarbon peaks of CH_3^+ , C_2H_5^+ and C_3H_7^+ . For the purposes of the test, and to optimize the Matsuda voltage, each mass spectrum should be acquired while varying only the Matsuda voltage by e.g. 5 V steps. The same acquisition time should be used for each

subsequent acquisition, and each mass spectrum must be calibrated following each acquisition.

Following each acquisition and calibration of the mass spectrum, the mass accuracy of atomic species (e.g. Na^+ , Mg^+ , Al^+ , Si^+ , etc.) and of unsaturated hydrocarbon species (e.g. C^+ , CH^+ , CH_2^+ and CH_3^+) must be measured. The mass accuracy may be obtained from the mass deviation column in the Peak ID tool. Note the sign and the magnitude of the mass deviation, as well as the mass resolution, for each measured secondary ion species. Following the measurements, the mass deviation for each secondary ion species should be plotted versus the Matsuda voltage. A 10 – 20 V range of the Matsuda voltage should be quite evident from the plot wherein both mass accuracy and mass resolution are optimized.

After completing the procedure for the positive secondary ion polarity (+SIMS), the same procedure should be repeated for the negative secondary ion polarity (-SIMS). Again, ensure that the sample bias is correct; the sample Z-height having already been set in the +SIMS should be optimal. The fully saturated, low mass hydrocarbon peaks of CH_3^- , C_2H_5^- and C_3H_7^- that are to be used for mass spectral calibration will have a much lower intensity and so more time will be necessary in order to obtain useful

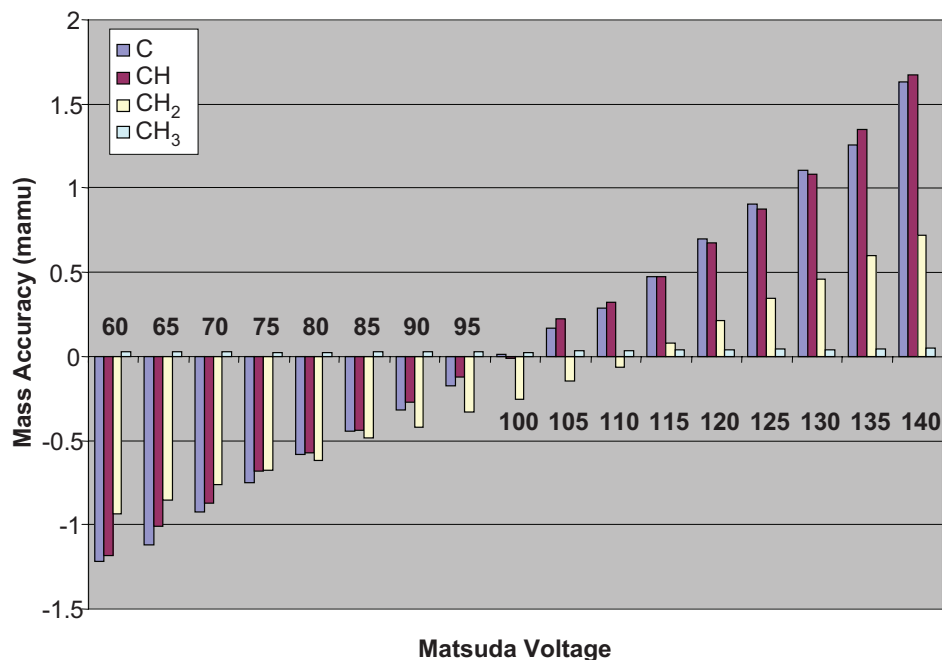


Figure 2: Mass accuracy as a function of Matsuda voltage for the hydrocarbon-based (i.e. molecular) secondary ions of C^+ , CH^+ , CH_2^+ and CH_3^+ . The data indicates the best mass accuracy to occur at a Matsuda voltage of approximately 100 V; however, the mass accuracy is less than 1 mamu over the range of 70 – 125 V.

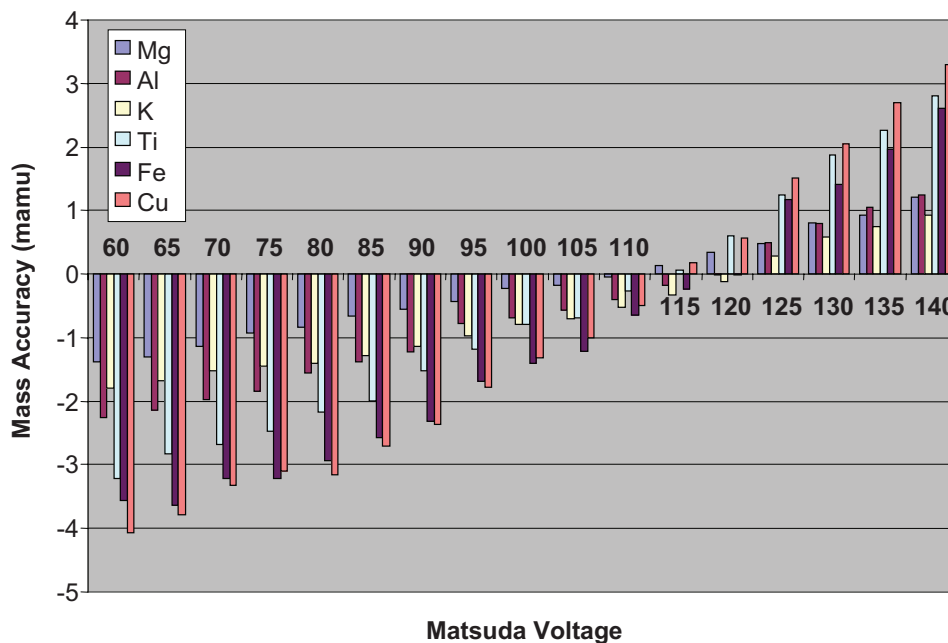


Figure 3: Mass accuracy as a function of Matsuda voltage for atomic (i.e. elemental) secondary ions of Mg^+ , Al^+ , K^+ , Ti^+ , Fe^+ and Cu^+ . The data indicates the best mass accuracy to occur at a Matsuda voltage of approximately 115 V; the mass accuracy is less than 1 mamu over a narrow range of 110 – 120 V.

counting statistics. Additionally, the atomic species used to determine mass accuracy as a function of Matsuda voltage will be different, e.g. O^- , F^- , Si^- , S^- , Cl^- , etc. The intensities of unsaturated hydrocarbon species (e.g. C^- , CH^- and CH_2^- , with the exception of CH_3^-) should be relatively strong.

Once the optimum values for the Matsuda voltage have been determined for both the +SIMS and the -SIMS polarities, these values should be saved into the Instrument State (INS) files.

RESULTS

An example data set for mass accuracy as a function of Matsuda voltage is rendered in Figures 2 and 3. Figure 2 is a histogram for the mass accuracies of unsaturated hydrocarbon species as a function of Matsuda voltage. From the histogram, the optimum Matsuda voltage is observed at approximately 100 V. However, note that the mass accuracy for these unsaturated hydrocarbon species remains below 1 mamu between 70 V and 125 V. Figure 3 is a histogram plot of the mass accuracies of atomic species as a function of Matsuda voltage. The optimum Matsuda voltage is observed at approximately 115 V; the mass accuracy remains below 1 mamu over a much smaller range of Matsuda voltage between 110 V and 120 V. Thus, the limiting criterion for achieving high mass accuracy

simultaneously for atomic and molecular species is that of the atomic species. If the Matsuda voltage is set in the range of 110 – 115 V then the mass accuracy of both the atomic and the molecular species remains well below 1 mamu.

Figure 4 is a plot of mass resolution for atomic and molecular species as a function of Matsuda voltage. The mass resolution of atomic species is inherently lower than that of molecular species due to the intrinsically broader kinetic energy spread of atomic secondary ions that results from the physics of secondary ion generation, i.e. the ion-solid interaction and the secondary ion trajectories. The kinetic energy distribution of monatomic and polyatomic secondary ions is illustrated in Figure 1. The data of Figure 4 indicates that the mass resolution is optimized for a Matsuda voltage in the range of 100 – 105 V. The mass accuracy, as discussed above, is optimized at a Matsuda voltage in the range of 110 – 115 V. Therefore, a slight decrease in mass resolution is realized in order to optimize the mass accuracy, but the mass resolution is only decreased by approximately 3%.

As discussed above, the kinetic energy distribution of atomic secondary ions is quite broad. This fact is related to the sputtering process, i.e. the ion-solid interaction resulting in secondary ion desorption, and the large angular distribution of the atomic secondary ions [2,3].

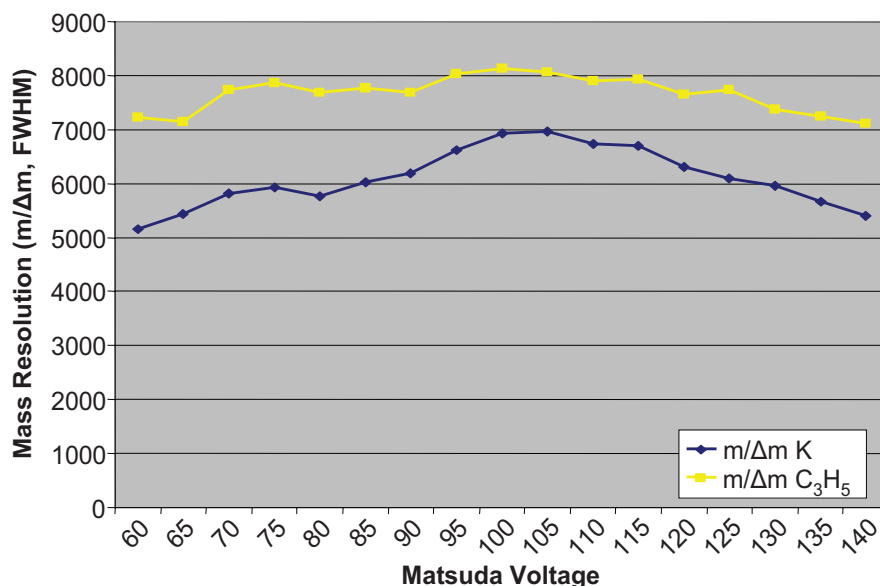


Figure 4: Illustration of mass resolution as a function of Matsuda voltage for atomic (i.e. elemental) secondary ions (blue, K^+) and hydrocarbon-based (i.e. molecular) secondary ions (yellow, $C_3H_5^+$).

The TRIFT spectrometer is highly efficient at collecting secondary ions having large (i.e. high off-normal) angular trajectories; the angular acceptance is effectively greater than 90° [4,5]. It is the large angular acceptance of the extraction optics that results in the capability of the TRIFT spectrometer to achieve both superior topographic imaging and secondary ion transmission. Because the kinetic energy distribution of the atomic species is large, the exceptional angular acceptance of the TRIFT spectrometer necessarily results in a modest reduction in the mass resolution of atomic secondary ions. However, the angular acceptance may be reduced to approximately 10° by moving the Contrast Diaphragm to the In position (i.e. CD-In) to achieve a mass resolution that is equivalent to that of the molecular species.

CONCLUSION

Tuning the Matsuda voltage of the TRIFT spectrometer may be accomplished such that high mass accuracies (i.e. less than 1 $mamu$ @ below 100 m/z) are achieved for both atomic and molecular secondary ions while simultaneously achieving high mass resolution for these secondary ion species. High mass resolution and mass accuracy are requisite in order to uniquely identify a peak in the mass spectrum

and to elucidate its composition. In addition to achieving high mass resolution and mass accuracy, the extraction optics of the TRIFT spectrometer feature an inherently large angular acceptance resulting in unequalled performance for secondary ion transmission and imaging of topographically rough specimens. The angular acceptance of atomic secondary ions may be moderated by the Contrast Diaphragm to achieve equivalent (i.e. high) mass resolution for both atomic and molecular secondary ions.

REFERENCES

- [1] T. Sakurai, Y. Fujita, T. Matsuo, H. Matsuda, I. Katakuse and K. Miseki, *Int. J. Mass Spectrom. Ion Proc.* **66** (1985) 283.
- [2] S. Sun, C. Szakal, N. Winograd and A. Wucher, *J. Am. Soc. Mass Spectrom.* **16** (2005) 1677.
- [3] Z. Postawa, B. Czerwinski, M. Szewczyk, E. Smiley, N. Winograd and B. Garrison, *J. Phys. Chem.* **B108** (2004) 7831.
- [4] J. Lee, I. Gilmore, I. Fletcher and M. Seah, *Appl. Surf. Sci.* **255** (2008) 1560.
- [5] *Quantitative Analysis of Topographic Effects on Conductive Surfaces*, Technical Bulletin (2009) Physical Electronics.

Physical Electronics

18725 Lake Drive East,
Chanhassen, MN 55317
952-828-6200
www.phi.com

ULVAC-PHI, Inc.

370 Enzo, Chigasaki,
Kanagawa, 253-8522,
Japan
81-467-85-4220
www.ulvac-phi.co.jp



PHYSICAL
ELECTRONICS